

Models for thin viscous sheets

P.D. Howell

Mathematical Institute, 24-29 St Giles', Oxford, UK

Abstract

Leading-order equations governing the dynamics of a two-dimensional thin viscous sheet are derived. The inclusion of inertia effects is found to result in an ill-posed model when the sheet is compressed, and the resulting paradox is resolved by rescaling the equations over new length- and timescales which depend on the Reynolds number of the flow and the aspect ratio of the sheet. Physically this implies a dominant lengthscale for transverse displacements during viscous buckling. The theory is generalised to give new models for fully three-dimensional sheets.

1 Introduction

In this paper we derive, via systematic asymptotic methods, equations governing the leading-order dynamics of thin viscous sheets. Our asymptotic methods are analogous to those applied to the flow of inviscid jets and sheets by Ting & Keller (1990), and to viscosity-dominated flow in slender axisymmetric fibres by Schultz & Davis (1982) and Dewynne, Ockendon & Wilmott (1989), for example. We illustrate them in section 2.1, while deriving the so-called Trouton model for the stretching of a purely two-dimensional sheet. Our principal aim is to show how the same techniques can be generalised to apply to sheets of arbitrary geometry, based only on the assumption that the inverse aspect ratio (the ratio of a typical thickness to a typical length) is small. This part of our work is therefore in the same spirit as that of Dewynne, Ockendon & Wilmott (1992), in which systematic asymptotic methods are applied to nonaxisymmetric viscous fibres. Our secondary aim is to incorporate inertia into the classical model and to illustrate the dramatic consequences for the behaviour of the solutions.

Purely viscous two-dimensional sheets have been considered by Buckmaster, Nachman & Ting (1975) (referred to hereafter as BNT) and Wilmott (1989), and the onset of buckling in a two-dimensional sheet impinging on a plate is considered by Yarin & Tchavdarov (1994). The linear stability of a viscous sheet subjected to shear was treated by Benjamin & Mullin (1988). Models for axisymmetric viscous sheets have been derived by Pearson & Petrie (1970) and Yarin, Gospodinov, & Roussinov (1994). A fully nonlinear model for the evolution of a three-dimensional sheet of arbitrary geometry has been derived by Howell (1994) and applied to the blowing of glass sheets by van de Fliert, Howell & Ockendon (1995).

In section 2 we review BNT's theory of inertia-free, two-dimensional viscous sheets. This theory predicts physically plausible behaviour for three distinct aspects of thin sheet

dynamics: the buckling of a sheet under compression, the straightening of an initially curved sheet under tension, and the evolution of a straight sheet as it stretches under tension.

In section 3 we show that this theory may be invalid when inertia effects are included in the model, even when the relevant Reynolds number is relatively small. We derive a model for the evolution of the centre-line of a viscous sheet, including inertia, which becomes ill-posed when the sheet is put under compression. However, this ill-posedness is only a manifestation of an incorrect choice of length- and timescales; the principal result of section 3 is to identify and implement the correct rescaling, which depends on the Reynolds number and the aspect ratio of the sheet.

In section 4 we generalise the two-dimensional theory of the previous two sections, and hence obtain models for fully three-dimensional sheets.

In the appendix we incorporate surface tension into the models derived in the paper.

2 Two-dimensional inertia-free sheets

2.1 The Trouton model

In this section we describe briefly the derivation, using systematic asymptotic expansions, of the simplest and most widely-known model for the extension of a thin viscous sheet. The derivation is straightforward, and indeed the governing equations (10) and (13) can be written down almost immediately via simple mass- and force-balances combined with physically plausible assumptions. However, we aim to use this simple example as a demonstration of our asymptotic methods; in the more complicated models to follow, we will largely omit the details of the derivations, which are conceptually similar to those employed in this section, though they frequently involve much more onerous algebraic manipulation.

Our starting point is the two-dimensional slow flow of a Newtonian fluid of constant viscosity between two free surfaces given by $y = H(x, t) - \frac{1}{2}h(x, t)$ and $y = H(x, t) + \frac{1}{2}h(x, t)$ (see figure 1). Thus $y = H(x, t)$ is the equation of the centre-line of the sheet, and $h(x, t)$ is its thickness.

We suppose that typical lengths and velocities for the flow are L and U in the x -direction, and ϵL and ϵU in the y -direction, where $\epsilon \ll 1$, and consider a time-scale over which the fluid is moved a distance of order L in the x -direction, i.e. L/U . Thus, denoting the components of the fluid velocity by u and v , we nondimensionalise as follows:

$$\begin{aligned} x &= Lx', & y &= \epsilon Ly', \\ u &= Uu', & v &= \epsilon Uv', \\ H &= \epsilon LH', & h &= \epsilon Lh', \\ t &= (L/U)t', & p &= (\mu U/L)p'. \end{aligned} \tag{1}$$

Here, our scaling of H implies that the sheet is not only thin, but also nearly flat, *i.e.* that its dimensionless curvature is of order ϵ . In order to model a sheet whose curvature is non-negligible it is more practical to employ curvilinear coordinates fixed in the sheet; we discuss such an approach in section 2.3. There are many other self-consistent scalings that can be considered. For example, the analysis of Yarin & Tchavdarov (1994) relies

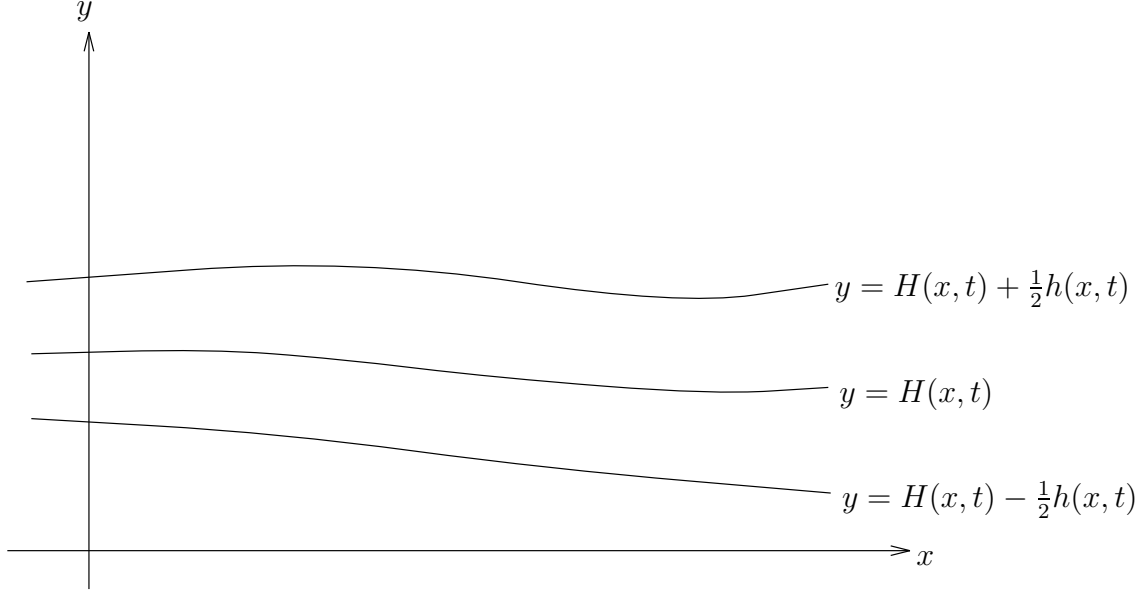


Figure 1: A two-dimensional sheet of fluid

on the assumption that H is an order of magnitude smaller than h , while Benjamin & Mullin (1988) consider disturbances whose wavelength is of the same order as h , but whose amplitude is an order of magnitude less. The relationship between the analysis of Benjamin & Mullin (1988) and the present work is analogous to the relationship between the theory of Stokes surface waves and shallow water theory in inviscid flow.

After this nondimensionalisation, the two-dimensional Stokes equations take the form

$$u_x + v_y = 0, \quad (2)$$

$$\epsilon^2 p_x = \epsilon^2 u_{xx} + u_{yy}, \quad (3)$$

$$p_y = \epsilon^2 v_{xx} + v_{yy}, \quad (4)$$

while the kinematic and (ignoring surface tension for the moment) dynamic boundary conditions on the two free surfaces read

$$v = H_t \pm \frac{1}{2} h_t + u \left(H_x \pm \frac{1}{2} h_x \right) \quad \text{on } y = H \pm \frac{1}{2} h, \quad (5)$$

$$\epsilon^2 (-p + 2u_x) \left(H_x \pm \frac{1}{2} h_x \right) = u_y + \epsilon^2 v_x \quad \text{on } y = H \pm \frac{1}{2} h, \quad (6)$$

$$(u_y + \epsilon^2 v_x) \left(H_x \pm \frac{1}{2} h_x \right) = -p + 2v_y \quad \text{on } y = H \pm \frac{1}{2} h. \quad (7)$$

We seek solutions of these equations and boundary conditions in the form of asymptotic expansions in powers of the small parameter ϵ^2 :

$$u \sim u_0 + \epsilon^2 u_1 + \epsilon^4 u_2 + \dots, \quad v \sim v_0 + \epsilon^2 v_1 + \epsilon^4 v_2 + \dots, \quad \text{etc.}$$

Formally setting $\epsilon = 0$ in (3) results in

$$u_{0_{yy}} = 0,$$

while the boundary condition (6) gives

$$u_{0y} = 0, \quad \text{on } y = H_0 \pm \frac{1}{2}h_0.$$

This problem for u_0 is homogeneous, and admits the eigensolution

$$u_0 = u_0(x, t), \tag{8}$$

that is, the axial velocity is uniform across the sheet; this type of flow is termed *extensional*. The transverse velocity may then be found from (2) :

$$v_0 = f(x, t) - yu_{0x},$$

where the arbitrary function f is found using the kinematic boundary condition (5), which gives

$$f(x, t) = H_{0t} \pm \frac{1}{2}h_{0t} + \left[u_0 \left(H_0 \pm \frac{1}{2}h_0 \right) \right]_x.$$

Hence

$$v_0 = H_{0t} + (u_0 H_0)_x - yu_{0x}, \tag{9}$$

and we obtain a relation between u_0 and h_0

$$h_{0t} + (u_0 h_0)_x = 0, \tag{10}$$

which represents conservation of mass. The leading-order pressure may be found from (2), (4) and (7),

$$p_0 = -2u_{0x}, \tag{11}$$

so that the leading-order dimensionless axial stress is

$$(\sigma_{xx})_0 = -p_0 + 2u_{0x} = 4u_{0x}. \tag{12}$$

We now have to consider the $O(\epsilon^2)$ terms in the expansions in order to derive a closed system of equations for the leading-order variables $h_0(x, t)$, $u_0(x, t)$ and $H_0(x, t)$. Equation (3) gives

$$u_{1yy} = -3u_{0xx}$$

with boundary conditions from (6),¹

$$u_{1y} = 4u_{0x} \left(H_{0x} \pm \frac{1}{2}h_{0x} \right) - H_{0xt} - (u_0 H_0)_{xx} + u_{0xx} \left(H_0 \pm \frac{1}{2}h_0 \right) \quad \text{on } y = H_0 \pm \frac{1}{2}h_0.$$

Note that in this problem for u_1 , the operator is the same as that in the problem for u_0 , though in this case there is an inhomogeneous right-hand side. As there exist eigenfunction solutions for u_0 , the Fredholm alternative implies that no solutions for u_1 exist unless an orthogonality condition is satisfied. In this case it is trivial to note that

$$\int_{H_0 - \frac{1}{2}h_0}^{H_0 + \frac{1}{2}h_0} u_{1yy} dy = [u_{1y}]_{H_0 - \frac{1}{2}h_0}^{H_0 + \frac{1}{2}h_0}$$

¹Note that we have omitted the identically zero term which arises from the expansion of H and h , namely $u_{0yy}(H_1 \pm \frac{1}{2}h_1)$. In general, terms arising from the expansion of the free surfaces should not be neglected, though it frequently transpires that they play no part in the leading-order equations.

and hence

$$(4h_0u_{0x})_x = 0, \quad (13)$$

which represents an axial force balance. We can then solve for u_{1y} , giving

$$u_{1y} = [4H_0u_{0x} - H_{0t} - (u_0H_0)_x]_x - 3yu_{0xx}. \quad (14)$$

Then (2) gives

$$v_{1yy} = [H_{0t} + (u_0H_0)_x - 4H_0u_{0x}]_{xx} + 3yu_{0xxx}, \quad (15)$$

(4) gives

$$p_{1y} = [2H_{0t} + 2(u_0H_0)_x - 4H_0u_{0x}]_{xx} + 2yu_{0xxx}, \quad (16)$$

and the boundary condition (7) reveals

$$-p_1 + 2v_{1y} = 4 \left(H_{0x} \pm \frac{1}{2}h_{0x} \right) \left[(H_0u_{0x})_x - u_{0xx} \left(H_0 \pm \frac{1}{2}h_0 \right) \right] \quad \text{on } y = H_0 \pm \frac{1}{2}h_0.$$

Then integration of $-p_{1y} + 2v_{1yy}$ between the two free surfaces gives a third leading-order equation, which reduces to

$$(4h_0u_{0x}H_{0x})_x = 0, \quad (17)$$

a lateral force balance.

We have left the factor 4 in (13) and (17) to emphasise the so-called ‘‘Trouton ratio’’ which is 4 for a two-dimensional Newtonian sheet. The significance is that $4h_0u_{0x}$ is the leading-order dimensionless tension in the sheet (see equation (12)).

Equations (10) and (13) form a hyperbolic system for the sheet thickness and the axial velocity, often known as the *Trouton Model*. It may readily be verified that the same model governs the leading-order cross-sectional area and axial velocity during the stretching of a slender axisymmetric viscous fibre, with a change in the Trouton ratio from 4 to 3; see, for example Dewynne *et al.* (1989), in which the general solution of the model is also found.

Equations (13) and (17) tell us that so long as the tension in the sheet is nonzero, H_0 is linear in x , so that the sheet’s centre-line is straight at this order, and without loss of generality,² we may take

$$H_0 = 0 \quad (18)$$

(*i.e.* in dimensional terms, we must have $H \sim \epsilon^2 L$, not $H \sim \epsilon L$ as is implicit in (1)). We are unable to satisfy the initial condition of a given H at $t = 0$, unless H is of order $\epsilon^2 L$ initially. This implies that the solution for H is a singular perturbation problem in t whose outer solution is $H = 0$ to leading order. In order to study the evolution of an initially curved centre-line, we must consider the inner solution for H , and hence use a timescale shorter than L/U . We discuss such a short timescale analysis in the next section.

If the ends of the fluid sheet are not pulled apart, but are pushed together, then in theory equations (10), (13) and (17) should still apply. However, it is clear experimentally that in this case an initially curved centre-line certainly will not straighten, and so equation (17) is false. The assumption that the centre-line is nearly straight ($H/L \ll 1$)

²This is because of the property of Stokes flow with a stress-free free surface that an arbitrary rigid-body motion may be added to the flow.

becomes invalid before times of order L/U are achieved, so the equations of this section cease to apply. Hence it is also necessary to consider a shorter timescale in order to study the “buckling” behaviour of a fluid sheet under compression.

2.2 The BNT model; $H \sim O(\epsilon L)$, $t \sim O(\epsilon^2 L/U)$

BNT found, by examining a short timescale of order $\epsilon^2 L/U$, an evolution equation for the centre-line of a two-dimensional sheet as it straightens under tension or buckles under compression. In our formulation this is achieved by rescaling the dimensionless Stokes equations and boundary conditions (2) to (7) over the new timescale:

$$t = \epsilon^2 \tau. \quad (19)$$

The kinematic boundary condition (5) implies that we should also rescale the transverse velocity v by setting

$$v = \epsilon^{-2} V. \quad (20)$$

Our method is, as in the previous section, to expand the dependent variables in powers of the small parameter ϵ^2 . As before it is necessary to proceed to higher order in the expansions in order to close the leading-order equations.

The Stokes equations and boundary conditions at leading order reveal that the transverse velocity V is independent of y . Hence the kinematic boundary condition gives (dropping subscripts)

$$V = H_\tau, \quad (21)$$

and

$$h_\tau = 0, \quad (22)$$

that is, the thickness of the sheet does not change with time. The leading-order axial velocity is given by

$$u = \bar{u}(x, \tau) + H_{x\tau}(H - y), \quad (23)$$

so that the leading-order flow is *not* purely extensional with the present scalings. The linear dependence of u on y leads to *bending* stresses in the sheet. With the scalings employed in section 2.1 we found that the dominant stress in the sheet was due to stretching; the bending stress was negligible to leading order. With the present scalings we find that stretching and bending stresses both play a part in the leading-order equations.

The solvability conditions for the $O(\epsilon^2)$ equations give the axial stress balance

$$4h(\bar{u}_x + H_x H_{x\tau}) = T(\tau), \quad (24)$$

which represents the tension in the sheet. Continuing to $O(\epsilon^4)$ in the analysis leads to the following equation for the centre-line of the sheet:

$$T(\tau)H_{xx} = \frac{1}{3}(h^3 H_{xx\tau})_{xx}. \quad (25)$$

BNT obtained equivalent equations by employing curvilinear coordinates fixed in the sheet. As we are only considering sheets with small curvature in this section, we have chosen to employ fixed Cartesian coordinates which simplify the analysis.

Over this short timescale the ends of the sheet do not move to leading order, and hence the end conditions for H may be applied at $x = 0$ and $x = 1$. If these end conditions are homogeneous then (25) can be solved by means of eigenfunction expansions:

$$H = \sum_{n=1}^{\infty} A_n f_n(x) \exp\left(-\frac{3}{\lambda_n^2} \int_0^{\tau} T(\tau') d\tau'\right), \quad (26)$$

where f_n and λ_n are the eigenfunctions and eigenvalues of

$$(h^3 f_n'')'' = \lambda_n^2 f_n'', \quad (27)$$

with the given homogeneous boundary conditions at $x = 0$ and $x = 1$. It is simple to establish that for reasonable h , the λ_n^2 are real and positive and that the f_n' are orthogonal and complete, so that the coefficients A_n may be found by Fourier analysis of $H_x(x, 0)$. For example, in the case considered by BNT in which $h = 1$ and $H = H_x = 0$ at the two ends of the sheet, we obtain

$$f_n(x) = 2 \sin(\lambda_n x) - \lambda_n \cos(\lambda_n x) - 2\lambda_n x + \lambda_n, \quad (28)$$

where the eigenvalues are the solutions of

$$\frac{\lambda_n}{2} = \tan\left(\frac{\lambda_n}{2}\right), \quad (29)$$

in agreement with the solution given by BNT. This separable solution implies that if the sheet is under compression ($T < 0$) then the solution grows exponentially in time and is dominated by the lowest mode, while if the sheet is under tension ($T > 0$) the solution decays exponentially, with the highest mode decaying slowest.

For cases where the boundary conditions imposed on H are inhomogeneous, (25) can still be solved by Laplace transform; this has been carried out by Wilmott (1989). The behaviour of the solutions that result is qualitatively similar to that of the separable solutions described above.

Not only have we rederived the results of BNT by a systematic perturbation procedure, but also we have revealed a decomposition of the behaviour of an inertia-free two-dimensional sheet into (i) bending without stretching and (ii) stretching without bending. We discuss this point further in section 2.4.

2.3 The BNT model; $H \sim O(L)$, $t \sim O(L/U)$

By considering a short timescale we have resolved the apparent paradox which we encountered in section 2.1, namely that the centre-line of the sheet was found to be straight to leading order. Equation (25) describes how an initially curved (but only by a distance of order ϵL) sheet will straighten under tension or buckle under compression over a timescale $\epsilon^2 L/U$. In the former case, the theory of section 2.1 becomes valid over a timescale L/U while in the latter case it is invalid as the displacement of the centre-line becomes large. Hence, in order to complete the picture, we now consider the dynamics of a two-dimensional sheet of non-negligible curvature.

The simplest way to derive the leading-order equations of motion is to employ curvilinear coordinates fixed in the sheet; this is the approach adopted by BNT. Here we describe briefly how equivalent equations may be derived using fixed Cartesian coordinates. Though this approach involves slightly more algebra, its advantage is that the analogy with the results of sections 2.1 and 2.2 is made clearer. The boundary conditions also take a simpler form in a fixed coordinate system.

We start with the two-dimensional Stokes equations and stress-free boundary conditions given in dimensionless form in (2) to (7). We then perform the following transformation,

$$y = H(\tilde{x}, \tilde{t}) + \tilde{y}, \quad v = H_{\tilde{t}} + uH_{\tilde{x}} + \tilde{v}, \quad x = \tilde{x}, \quad t = \tilde{t}, \quad (30)$$

which results in the chain rules

$$\frac{\partial}{\partial t} = \frac{\partial}{\partial \tilde{t}} - H_{\tilde{t}} \frac{\partial}{\partial \tilde{y}}, \quad \frac{\partial}{\partial x} = \frac{\partial}{\partial \tilde{x}} - H_{\tilde{x}} \frac{\partial}{\partial \tilde{y}}, \quad \frac{\partial}{\partial y} = \frac{\partial}{\partial \tilde{y}}. \quad (31)$$

After making the above transformation the leading-order equations of section 2.1 can be derived simply via the scalings

$$\begin{aligned} \tilde{x} &= L\tilde{x}', & \tilde{y} &= \epsilon L\tilde{y}', \\ u &= Uu', & \tilde{v} &= \epsilon U\tilde{v}', \\ H &= \epsilon LH', & h &= \epsilon Lh', \\ t &= (L/U)t', & p &= (\mu U/L)p'. \end{aligned}$$

Here, we are interested in large displacements of the centre-line and the only change needed to the above scalings is to nondimensionalise H with L instead of ϵL . Then we proceed to expand the unknowns in powers³ of ϵ . It is necessary to continue the expansions up to $O(\epsilon^2)$ and the algebra is fairly unpleasant so we proceed directly to the leading-order equations that result. These are (dropping primes and tildes)

$$h_t + (uh)_x = 0, \quad (32)$$

$$H_x(H_{xt} + uH_{xx}) + u_x(1 + H_x^2) = 0, \quad (33)$$

$$\left[\frac{h^3}{3(1 + H_x^2)^2} \left(\frac{H_{xt} + uH_{xx}}{1 + H_x^2} \right) \right]_{xx} = T(t)H_{xx}, \quad (34)$$

where the arbitrary function T represents the tension in the sheet (as in (13) and (24)). In the case where H is of order ϵL in dimensional variables, T is an order of magnitude larger than the left-hand side of (34), and hence the leading-order equation $H_{xx} = 0$ is recovered. Notice also that the short timescale equation (25) can be obtained by linearising these equations for small H .

Appropriate initial and boundary conditions are: given h and H at $t = 0$, and given u , H and H_x at the two ends of the sheet (say $x = 0$ and $x = x_1(t)$). It is also necessary to specify h at the ends of the sheet whenever fluid flows in; *i.e.* $h(0, t)$ must be given if $u(0, t) > 0$ and $h(x_1(t), t)$ must be given if $u(x_1(t), t) < \dot{x}_1(t)$.

³Note that here it is necessary to consider powers of ϵ while in sections 2.1 and 2.2 our expansions were in powers of ϵ^2 (that is we were free to choose all coefficients of odd powers of ϵ to be zero).

Equations (32), (33) and (34) take a more familiar form when recast in the curvilinear coordinates employed by BNT. We denote by α the angle made by the centre-line of the sheet with a fixed horizontal axis, and by s arc length along the centre-line, so that

$$H_x = \tan \alpha, \quad \frac{\partial}{\partial s} = \cos \alpha \frac{\partial}{\partial x}.$$

We also note that h is the thickness of the sheet, *as measured in the y -direction*; the thickness of the sheet as measured in the normal direction is given by

$$\tilde{h} = h \cos \alpha.$$

Hence (32) and (33) combine to give

$$\tilde{h}_t = 0, \tag{35}$$

(here $\partial/\partial t$ represents differentiating with respect to t while holding s constant) so that there is no stretching of the sheet to leading order, and (34) becomes

$$\left(\tilde{h}^3 \alpha_{st} \right)_s = F(t) \cos \alpha + G(t) \sin \alpha. \tag{36}$$

This is the so-called “viscida” equation derived by BNT. If the time-derivative on the left-hand side were not present it would be identical to the elastica equation of linear elasticity. It is nonlinear and in general must be solved by numerical means. Notice that though (36) takes a somewhat simpler form than (34) (particularly as \tilde{h} is a known function of s), the boundary conditions for H outlined above translate into: given α at the two ends of the sheet, along with two integral conditions for α (see BNT for details). Using these four conditions, the arbitrary functions F and G can be found and (36) can be solved in principle.

2.4 Summary

The theory of inertia-free two-dimensional viscous sheets may be summarised as follows.

- A sheet of $O(\epsilon L)$ thickness and $O(L)$ displacement, when put under tension by moving its ends with a relative speed of order U , straightens over a timescale $O(L/U)$, *without stretching*. The motion of the sheet is governed by (36).
- When the displacement reaches $O(\epsilon L)$, the sheet subsequently straightens over a timescale $O(\epsilon^2 L/U)$, again without stretching. The displacement of the centre-line is given by (25), which predicts that the smallest wavelength modes are the slowest to decay.
- Once the sheet has straightened, it stretches over a timescale $O(L/U)$, satisfying the Trouton model.
- When a nearly straight sheet (with thickness and displacement both of order ϵL) is compressed by moving its ends towards each other with relative speed U , it buckles over a timescale $O(\epsilon^2 L/U)$. During the motion, there is no stretching, the governing equation is (25) and the longest wavelength modes dominate.

- When the displacement of the centre-line becomes of order L , the buckling continues over a timescale L/U , there is no stretching, and the motion of the sheet is governed by (36).

For example, to model the buckling of an initially nearly straight sheet under given end conditions, one would first solve the linear problem (25). The dominant behaviour of this solution as $\tau \rightarrow \infty$ would then be used as the initial condition for a numerical integration of (36). This is the approach which was adopted by BNT.

Note that (25) and (34) are both invariant under the transformation $\{\tau \rightarrow -\tau, T \rightarrow -T\}$. Hence the model predicts that the motion of the sheet is reversible. One aspect of this is that short-wavelength displacements grow the most slowly during buckling and take the longest time to decay during straightening of the sheet. In practice, or indeed during a numerical integration of the equations over a long time interval, short-wavelength disturbances will be lost during straightening because of dampening effects and the lowest buckling mode will dominate during compression, so this mathematical reversibility will be of academic interest.

3 Inertia effects

We now describe the dramatic effect that the incorporation of inertia effects has on the theory of the previous section. The inclusion of inertia results in the introduction of a dimensionless parameter, the Reynolds number,

$$Re = \frac{\rho UL}{\mu},$$

into the problem. We may expect the behaviour of our model to depend critically on the size of the Reynolds number compared to our small parameter ϵ . We consider three representative examples: $Re = O(1)$, $Re = O(\epsilon^2)$ and $Re = O(\epsilon^4)$ (to get some idea of how relevant these may be in practice, in the “float glass” process for the manufacture of plate glass, the viscous sheets involved typically have an inverse aspect ratio of 10^{-3} or less, while the Reynolds number can vary from 10^{-10} to 10^{-2}).

3.1 The Trouton model with inertia; $Re \sim O(1)$

The methods of section 2.1 may be applied to the more general case when inertia effects are significant, by considering the full Navier–Stokes equations in place of the Stokes equations. Treating Re as an order one constant, the resulting leading-order equations are found to be (dropping subscripts)

$$h_t + (uh)_x = 0, \quad (4hu_x)_x = Reh(u_t + uu_x), \quad (37)$$

with the decoupled equation for H ,

$$(Reu^2 - 4u_x)H_{xx} + 2ReuH_{xt} + ReH_{tt} = 0. \quad (38)$$

Analogous equations were found to apply to a slender nonaxisymmetric viscous fibre with inertia by Dewynne *et al.* (1994). These equations are much more difficult to solve than

the standard Trouton model. However, several general statements may be made about the properties which are introduced due to inertia effects:

- three more initial conditions are required by this system than in the inertia-free case;
- the short timescale analysis of section (2.2) is redundant if the Reynolds number is this large; indeed, (38) suggests that any short timescale analysis will simply give $H_{tt} = 0$ as the governing equation for the centre-line;
- the equations no longer have the reversibility properties noted at the end of section 2.4; indeed, the equation for the centre-line changes type from hyperbolic to elliptic depending on whether the sheet is under tension ($u_x > 0$) or compression ($u_x < 0$);
- the hyperbolic case will give rise to wave-like behaviour, while the elliptic case is ill-posed in the sense of Hadamard, leading to blow-up with the linearised growth rate becoming unbounded as the spatial wavenumber tends to infinity; we discuss in section 3.4 how this pathological behaviour is prevented from occurring in practice.

For many industrial applications, the Reynolds number will typically be much less than $O(1)$. However, (38) implies that inertia effects may still be significant over a timescale $t = O(Re^{1/2})$.

3.2 Short timescale analysis with $Re \sim O(\epsilon^2)$

We now consider the case, relevant to many processes, in which Re is of order ϵ^2 . In this case, inertia plays no part in the leading-order equations over the timescale L/U , and the equations of section 2.1 are recovered. As in section 2.2, we would like to consider a short timescale in order to model the evolution of a sheet which is not straight initially. However, with the present scaling of the Reynolds number, the timescale $t = O(\epsilon^2)$ used in section 2.2 is no longer relevant; the timescale over which viscous and inertia effects are balanced is $t = O(\epsilon)$.

We put

$$Re = \epsilon^2 Re',$$

assuming $Re' = O(1)$, and nondimensionalise the two-dimensional Navier–Stokes equations and stress-free boundary conditions according to

$$\begin{aligned} x &= Lx', & y &= \epsilon Ly', \\ u &= Uu', & \tilde{v} &= Uv', \\ H &= \epsilon LH', & h &= \epsilon Lh', \\ t &= (\epsilon L/U)t', & p &= (\mu U/L)p', \end{aligned}$$

where the scaling for v is motivated by the kinematic boundary condition. After applying these scalings, we drop primes and seek solutions in the form of asymptotic expansions in powers of ϵ . The analysis is relatively straightforward, and results in the leading-order equations (dropping subscripts)

$$h_t = 0, \quad 4hu_x = T(t), \quad T(t)H_{xx} = Re'hH_{tt}. \quad (39)$$

The dependence of the type of the centre-line equation on the sign of T is clear. Notice that (39) can be obtained directly by formally rescaling t in (38).

As in section 2.2, the end conditions for H are applied at $x = 0$ and $x = 1$, since the ends of the sheet do not move over this timescale to leading order. If these conditions are homogeneous, the solution for H can be expanded in the form

$$H = \sum_{n=1}^{\infty} f_n(x) (a_n g_{1,n}(t) + b_n g_{2,n}(t)), \quad (40)$$

where f_n are the eigenfunctions of the Sturm–Liouville equation

$$f_n'' + \lambda_n^2 Re' h f_n = 0, \quad (41)$$

which satisfy the given conditions at $x = 0$ and $x = 1$, and $g_{1,n}$ and $g_{2,n}$ are the two linearly independent solutions of

$$g_n'' + \lambda_n^2 T g_n = 0. \quad (42)$$

The coefficients a_n and b_n are found by Fourier analysis of $H(x, 0)$ and $H_t(x, 0)$.

Consider, for example, the steady state solution of (10), (13) and (17), namely

$$h = h_0 e^{-cx}, \quad T = \text{const.}, \quad H = 0.$$

We can examine the response of the centre-line to small disturbances over our short timescale by substituting for h and T into (39). Assume the end conditions are $H = 0$ at $x = 0$ and $x = 1$, and without loss of generality, so long as T is positive, we may suppose the equations are scaled in such a way that $h_0 = T = 1$. Then the general solution for H is

$$H = \sum_{n=1}^{\infty} \left(J_0(\gamma_n) Y_0(\gamma_n e^{-cx/2}) - J_0(\gamma_n e^{-cx/2}) Y_0(\gamma_n) \right) (a_n \cos(\omega_n t) + b_n \sin(\omega_n t)), \quad (43)$$

where the eigenvalues γ_n are the roots of

$$J_0(\gamma_n) Y_0(\gamma_n e^{-c/2}) - J_0(\gamma_n e^{-c/2}) Y_0(\gamma_n) = 0,$$

and $\omega_n = c\gamma_n/(2\sqrt{Re})$. If T is negative, the oscillatory terms in t become exponentials and the pathological behaviour alluded to earlier is clear: the growth rate of the modes becomes unbounded as their wavelength goes to zero. We will discuss in section 3.4 how this blow-up is prevented from occurring in practice.

3.3 Short timescale analysis with $Re \sim O(\epsilon^4)$

We now examine the case in which $Re = O(\epsilon^4)$ so that the inertial timescale of $Re^{1/2}$ is the same as the ϵ^2 timescale used in section 2.2. We put

$$Re = \epsilon^4 Re^*,$$

and employ the same nondimensionalisations as those in section 2.2. The result is, as may have been anticipated, equations similar to those of section 2.2 with an additional term due to inertia. These are

$$h_\tau = 0, \quad (44)$$

$$4h(\bar{u}_x + H_x H_{x\tau}) = T(\tau), \quad (45)$$

$$T(\tau)H_{xx} = \frac{1}{3}(h^3 H_{xx\tau})_{xx} + Re^* h H_{\tau\tau}. \quad (46)$$

The appearance of the higher derivative of H in (46) means that it is no longer ill-posed when T is negative. We do not discuss the solution of these equations, but simply make the observation that if the Reynolds number is not less than $O(\epsilon^4)$ then inertia effects cannot be ignored when considering the short timescale behaviour of a fluid sheet. It seems likely that this will be the case for many relevant industrial applications.

3.4 Regularisation of the ill-posed problems

In this section we discuss how elements of the inertia-free theory and the theory incorporating inertia may be combined to make sense of the unphysical pathological behaviour which is predicted when the sheet is put under compression. Notice that the ill-posed equations (38) and (39) when $T < 0$ predict the dominance of short lengthscale displacements as the sheet buckles. If x is rescaled to examine such a short lengthscale, we may expect the $(h^3 H_{xx\tau})_{xx}$ term of equation (25) to become important and hence regularise the equation.

This motivates us in the case $T < 0$ to examine the consequences of rescaling x as well as t . To determine the important length- and timescales, we start by considering the simplified paradigm centre-line equation, motivated by (46),

$$TH_{xx} = \frac{\epsilon^2}{3}H_{xxxxt} + ReH_{tt}, \quad (47)$$

where we have assumed that, over the length- and timescales we will be considering, variations in h and T may be neglected. We find the linear growth rates by looking for a solution of the form

$$H = H_0 e^{ikx + \lambda t},$$

which, on substitution into (47) gives

$$\lambda = \frac{-\epsilon^2 k^4 \pm k\sqrt{\epsilon^4 k^6 - 36ReT}}{6Re}. \quad (48)$$

Here, λ is the linear growth rate and $k = L/\tilde{L} > 1$, where L is the length of the sheet and \tilde{L} is the lengthscale of the disturbance. When $T < 0$, there is always one positive root for λ , so that all modes grow exponentially. However, the growth rate tends to zero like $-3T/(\epsilon^2 k^2)$ as $k \rightarrow \infty$, and there is a maximum value for λ , and hence a dominant lengthscale, given by

$$\frac{\tilde{L}}{L} \sim O(\epsilon^{2/3} Re^{-1/6}), \quad (49)$$

with linear growth rate

$$\lambda \sim O(\epsilon^{-2/3} Re^{-1/3}). \quad (50)$$

Notice that if $Re < O(\epsilon^4)$ then this length is greater than the length of the sheet and so the dominant lengthscale is L , with the corresponding linear growth rate of order ϵ^{-2} ; this agrees with the inertia-free theory of section 2.2. However, if $Re > O(\epsilon^4)$ then (49) and (50) give the lengthscale of the disturbances whose amplitude grows the fastest and the timescale over which they grow. This dominant lengthscale increases as the Reynolds number decreases, while the corresponding timescale decreases.

Note that, while \tilde{L} is the appropriate lengthscale for disturbances to the centre-line $y = H$, variations in h and u still take place over a lengthscale L . Hence in general, it is necessary to perform a two-lengthscale analysis.

As a simple example, consider the case (chosen to make the scalings as simple as possible) in which $Re = O(\epsilon)$. This means that over the usual lengthscale and timescale inertia does not enter the leading-order equations, which are therefore identical to those of section 2.1. If only time is rescaled, over the inertial timescale $Re^{1/2} \sim \epsilon^{1/2}$, then leading-order equations identical to those obtained in section 2.2 (for $Re = O(\epsilon^2)$) result. The centre-line equation is ill-posed if the sheet is under compression.

Using the ideas of this section, we may rescale both x and t ; from (49), the appropriate new lengthscale is given by $\tilde{L}/L = \epsilon^{1/2}$, and the short timescale implied by (50) is $t = O(\epsilon L/U)$. Hence we set $Re = \epsilon \tilde{Re}$ and scale the Navier-Stokes equations via the following nondimensionalisations:

$$\begin{aligned} x &= Lx', & y &= \epsilon Ly', \\ u &= Uu', & v &= Uv', \\ H &= \epsilon LH', & h &= \epsilon Lh', \\ t &= (\epsilon L/U)t', & p &= (\mu U/L)p'. \end{aligned}$$

We also introduce a short lengthscale, denoted by

$$\xi = \epsilon^{-1/2}x,$$

and, in order to perform a two-lengthscale analysis, treat x and ξ as independent, so that partial x -derivatives become:

$$\frac{\partial}{\partial x} = \frac{1}{L} \left(\frac{\partial}{\partial \tilde{x}} + \frac{1}{\epsilon^{1/2}} \frac{\partial}{\partial \xi} \right).$$

After these rescalings, we expand the Navier-Stokes equations in powers of $\epsilon^{1/2}$. After some algebra, the centre-line is found to satisfy

$$TH_{\xi\xi} = \left(\frac{h^3}{3} H_{\xi\xi t} \right)_{\xi\xi} + \tilde{Re} h H_{tt}, \quad (51)$$

where the tension T is a function of x and t , while the thickness h is a function only of x and ξ .

This example demonstrates how, by rescaling x as well as t , elements of the inertia-free theory and of the theory including inertia can be combined, and hence the catastrophic change of type caused by the inclusion of inertia can be avoided.

3.5 Discussion

In section 2 we showed that, by considering a timescale of order $\epsilon^2 L/U$ as well as the standard timescale of L/U , a complete, self-consistent model can be formulated to describe the buckling under compression or straightening and stretching under tension of a two-dimensional inertia-free sheet. However, in this section we have shown that inertia effects may invalidate this model even when the Reynolds number is relatively small, since their importance increases over short timescales. In order to provide a self-consistent model which includes inertia effects we found that it is necessary to introduce a new short lengthscale, dependent on the size of the Reynolds number, as well as a short timescale.

To reiterate, the practical implication of our theory is that a two-dimensional sheet, when put in compression with a Reynolds number $Re > O(\epsilon^4)$, will be most unstable to disturbances on a length-scale of order $L\epsilon^{2/3}Re^{-1/6}$.

Note that in many practical situations it is not necessary to know the details of the short-timescale dynamics. For example, in order to model fibre tapering, we only need to know that the fibre will instantaneously straighten when it is placed under tension; the manner in which it does so is largely irrelevant. In the following section, in which we present models for fully three-dimensional viscous sheets, we therefore do not pursue short timescale analyses explicitly, though we make some conjectures about what the results of such analyses might be.

4 Generalisation to three-dimensional sheets

We now show how the models for two-dimensional sheets developed in section 2 may be generalised to describe sheets which vary in two directions. In section 4.1 we generalise the Trouton model of section 2.1 to a two-dimensional model for the stretching of a viscous sheet. In section 4.2 we consider the transverse motion of a viscous sheet; this turns out to be analogous to the short timescale analysis of section 2.2. Then in section 4.3 we present a model for a viscous sheet with non-negligible curvature.

4.1 The “viscous sheet” equations

As in section 2.1, we start by considering the flow of an inertia-free viscous sheet of constant viscosity. Now we denote the centre-surface of the sheet by $z = H(x, y, t)$ and the thickness by $h(x, y, t)$. If L is a typical length in the x - and y -directions, then our asymptotic analysis is based on the assumptions that H/L and h/L are both everywhere much smaller than 1. For the moment we also assume that the fluid velocity is principally in-plane, so that the horizontal velocity components are typically larger by a factor of ϵ^{-1} than the transverse velocity. We omit the derivation of the leading-order equations which is analogous to that given in section 2.1 for a purely two-dimensional sheet.

In section 2.1 we found that the leading-order flow was extensional, that is the axial velocity was uniform across the sheet. For the fully three-dimensional sheet, this generalises to the fact that both tangential velocity components are independent of z to leading order: (neglecting subscripts)

$$u = u(x, y, t), \quad v = v(x, y, t). \quad (52)$$

Our generalisation of the conservation of mass equation (10) is

$$h_t + (uh)_x + (vh)_y = 0. \quad (53)$$

Instead of the single axial force balance (13) we obtain two tangential stress balances, namely

$$\left. \begin{aligned} [2h(2u_x + v_y)]_x + [h(u_y + v_x)]_y &= 0 \\ [h(u_y + v_x)]_x + [2h(u_x + 2v_y)]_y &= 0 \end{aligned} \right\} \quad (54)$$

while the centre-surface of the sheet satisfies the decoupled equation (a generalisation of (17)),

$$(2u_x + v_y)H_{xx} + (u_y + v_x)H_{xy} + (u_x + 2v_y)H_{yy} = 0. \quad (55)$$

Equation (53) is a hyperbolic equation for h whose characteristics are streamlines. Hence suitable boundary and initial conditions are for h to be given at $t = 0$, and along any edge of the fluid sheet where the fluid flows *in*. The system (54) for u and v has two pairs of repeated imaginary characteristics (similar to the biharmonic equation). Hence it is necessary to give two boundary conditions for u and v on the whole of the boundary of the fluid sheet.

For a purely two-dimensional sheet, (55) implies that the centre-line is straight, as we observed in section 2.1. However, in this more general case, a wide variety of behaviours of H is possible. Indeed, the type of (55), and hence the kind of boundary conditions which must be imposed on H , depends on the stresses that are induced in the fluid sheet.

To make this clearer, consider a local solution of (53) and (54) near a point which we may take as the origin, in the form

$$\begin{aligned} h &\sim h(0, 0, t) + \dots, \\ u &\sim u(0, 0, t) + xu_x(0, 0, t) + yu_y(0, 0, t) + \dots, \\ v &\sim v(0, 0, t) + xv_x(0, 0, t) + yv_y(0, 0, t) + \dots \end{aligned}$$

After elimination of the rigid-body motion and a suitable rotation of the axes, the local behaviour of the velocity field may always be written in the form

$$u \sim \alpha x + \dots, \quad v \sim \beta y + \dots, \quad (56)$$

(*i.e.* the local velocity field is a combination of a rigid-body motion and two perpendicular extensions or compressions) where

$$h(0, 0, t) = h_0 \exp \left(- \int_0^t \alpha(\tau) + \beta(\tau) d\tau \right). \quad (57)$$

The local type of the centre-surface equation (55) is therefore determined by the sign of $(2\alpha + \beta)(\alpha + 2\beta)$; if it is positive (so that σ_{xx} and σ_{yy} have the same sign), (55) is elliptic, while if it is negative (so that σ_{xx} and σ_{yy} take different signs), then (55) is hyperbolic.

Unfortunately, except for trivial examples like that just considered, the nonlinear system (53) and (54) must be solved numerically. Only once the solution for u and v has been found can the right kind of boundary conditions to apply for H be determined. In general we must also anticipate situations in which one of the principal stresses changes sign, so that equation (54) changes type from elliptic to hyperbolic, along some line in the x - y plane; we may expect a weak singularity in H along such a “sonic” line

4.2 Transverse motion of a viscous sheet

In section 4.1 we derived a model for a viscous sheet which is both thin ($h/L \ll 1$) and nearly flat ($H/L \ll 1$). However, we also made one further assumption, namely that the fluid velocity is principally in the plane of the sheet. We now consider sheets whose velocity is principally transverse. The limitation of the theory to follow is that we can only expect it to be valid for a limited period of time while the sheet remains nearly planar; when this ceases to be the case it will be necessary to resort to the more complicated theory of the following section.

As before, we suppose that if a typical length-scale in the x - and y -directions is L , then the thickness of the sheet and the displacement of the centre-surface, given by $z = H(x, y, t)$ are both typically of order ϵL , where $\epsilon \ll 1$. Here, however, we suppose a typical velocity in the z -direction is V , and that the velocities in the x - and y -directions are an order of magnitude smaller, that is of order ϵV . Now when we consider a timescale $t \sim O(V/L)$, these scalings are identical to the “BNT” short-time scalings employed in section 2.2; the leading-order equations are therefore simply three-dimensional generalisations of equations (22), (23), (24) and (25), namely

$$h_t = 0, \quad (58)$$

$$u = \bar{u}(x, y, t) + H_{xt}(H - z), \quad v = \bar{v}(x, y, t) + H_{yt}(H - z), \quad (59)$$

$$\left. \begin{aligned} \frac{\partial \bar{\sigma}_{xx}}{\partial x} + \frac{\partial \bar{\sigma}_{xy}}{\partial y} &= 0 \\ \frac{\partial \bar{\sigma}_{xy}}{\partial x} + \frac{\partial \bar{\sigma}_{yy}}{\partial y} &= 0 \end{aligned} \right\}, \quad (60)$$

where the in-plane stresses are given by

$$\left. \begin{aligned} \bar{\sigma}_{xx} &= 2h[2(\bar{u}_x + H_x H_{xt}) + (\bar{v}_y + H_y H_{yt})] \\ \bar{\sigma}_{xy} &= h[(\bar{u}_y + H_y H_{xt}) + (\bar{v}_x + H_x H_{yt})] \\ \bar{\sigma}_{yy} &= 2h[(\bar{u}_x + H_x H_{xt}) + 2(\bar{v}_y + H_y H_{yt})] \end{aligned} \right\}, \quad (61)$$

and the equation for the centre-surface of the sheet,

$$\bar{\sigma}_{xx} H_{xx} + 2\bar{\sigma}_{xy} H_{xy} + \bar{\sigma}_{yy} H_{yy} = \frac{1}{6}[h^3(2H_{xxt} + H_{yyt})]_{xx} + \frac{1}{3}[h^3 H_{xyt}]_{xy} + \frac{1}{6}[h^3(H_{xxt} + 2H_{yyt})]_{yy}. \quad (62)$$

As a simple example, suppose the sheet has uniform thickness initially. Then because of (58) we may set $h = 1$ for all time. As a result of (60) we may employ an Airy stress function \mathfrak{A} satisfying

$$\bar{\sigma}_{xx} = \mathfrak{A}_{yy}, \quad \bar{\sigma}_{xy} = -\mathfrak{A}_{xy}, \quad \bar{\sigma}_{yy} = \mathfrak{A}_{xx}. \quad (63)$$

For this simple case of uniform thickness, \bar{u} and \bar{v} may be eliminated from (61) to give the following equation for \mathfrak{A} :

$$\nabla^4 \mathfrak{A} + 3 \frac{\partial}{\partial t} (H_{xx} H_{yy} - H_{xy}^2) = 0, \quad (64)$$

and equation (62) for H reduces to

$$\mathfrak{A}_{yy}H_{xx} - 2\mathfrak{A}_{xy}H_{xy} + \mathfrak{A}_{xx}H_{yy} = \frac{1}{3}\nabla^4 H_t. \quad (65)$$

This nonlinear system for \mathfrak{A} and H is similar to the so-called von Kármán equations for a thin elastic plate (see, for example, Love (1927), article 335E). Indeed, the von Kármán equations may be obtained from (64) and (65) by deleting the time derivatives.

The system (64) and (65) has one real and eight imaginary characteristics; suitable boundary and initial conditions are given H at $t = 0$ along with two conditions each on H and \mathfrak{A} on the boundary of the sheet. This can be seen from the following proposed solution procedure:

- suppose at some instant of time H is known;
- solve (64) and (65) as a boundary value problem for \mathfrak{A} and H_t ;
- using the calculated H_t , update H .

The problem for \mathfrak{A} and H_t may be written in a symmetric form as follows. Set $w = H_t$ and define the self-adjoint operator \mathfrak{D}^2 by

$$\mathfrak{D}^2 f = H_{yy}f_{xx} - 2H_{xy}f_{xy} + H_{xx}f_{yy} = (H_{yy}f)_{xx} - 2(H_{xy}f)_{xy} + (H_{xx}f)_{yy}.$$

In terms of these, (64) and (65) take the form

$$\begin{aligned} \nabla^4 \mathfrak{A} + 3\mathfrak{D}^2 w &= 0, \\ \nabla^4 w - 3\mathfrak{D}^2 \mathfrak{A} &= 0. \end{aligned} \quad (66)$$

As a simple example of the behaviour we may expect of H , we return to the simple local solution introduced in section 4.1, namely

$$u = \alpha x, \quad v = \beta y, \quad h = \exp\left(-\int_0^t \alpha(\tau) + \beta(\tau) d\tau\right).$$

For simplicity suppose α and β are constant, and consider the response of a typical Fourier component,

$$H = e^{\lambda t} \cos[k(y \cos \theta - x \sin \theta)].$$

Substitution into (62) gives the following expression for the linearised growth rate:

$$\lambda = \frac{3}{k^2} ((\alpha - \beta) \cos(2\theta) - 3(\alpha + \beta)). \quad (67)$$

Hence all such Fourier modes decay if $\{2\alpha + \beta > 0, \alpha + 2\beta > 0\}$ (this corresponds to the steady-state equation being elliptic, with σ_{xx} and σ_{yy} both positive), all grow if $\{2\alpha + \beta < 0, \alpha + 2\beta < 0\}$ (this corresponds to the steady-state equation being elliptic, with σ_{xx} and σ_{yy} both negative), while there is a mixture of stable and unstable modes, depending on θ , in the case in which σ_{xx} and σ_{yy} are of opposite signs and the steady-state equation is hyperbolic. In all cases, the least stable modes are of long wavelength, and lie on the line $\theta = 0$ if $\alpha > \beta$ or $\theta = \pi/2$ if $\beta > \alpha$.

These cases are depicted schematically in figure 2. All modes are stable in region 1, all are unstable in region 2, while in regions 3 and 4 there are sectors of instability. The dashed line is $\alpha = \beta$; this separates the region in which the least stable modes lie on $\theta = 0$ from that in which they lie on $\theta = \pi/2$.

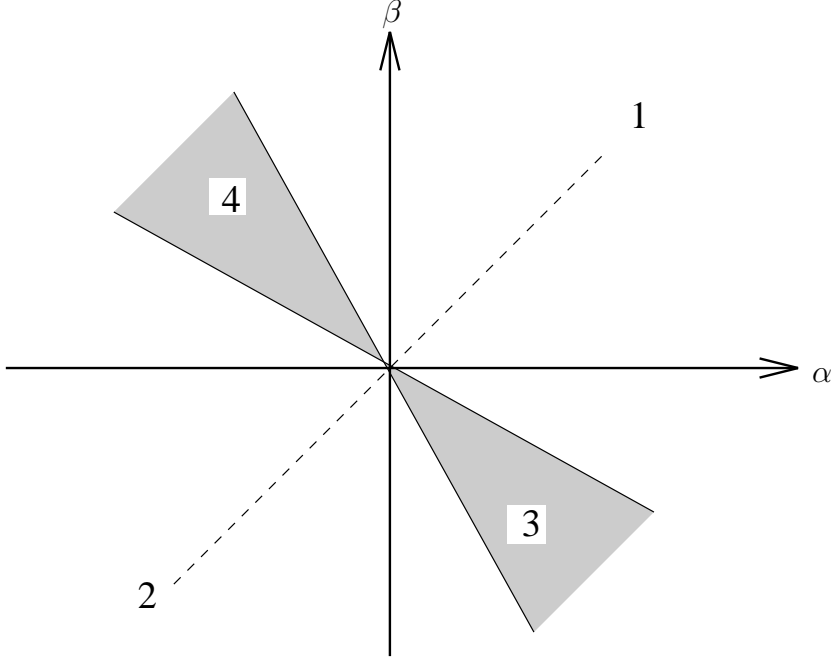


Figure 2: The (α, β) parameter space

4.3 The “viscous shell” equations

In this section we present a model for a fully three-dimensional viscous sheet of non-negligible curvature. As in section 2.3, the model is derived most simply by employing curvilinear coordinates fixed in the sheet. For the present problem, we suppose that the centre-surface of the sheet is given by

$$\mathbf{r} = \mathbf{r}_c(x_1, x_2, t),$$

where x_1 and x_2 are spatial parameters and t is time. The unit normal to this surface is given by

$$\mathbf{n} = \left| \frac{\partial \mathbf{r}_c}{\partial x_1} \wedge \frac{\partial \mathbf{r}_c}{\partial x_2} \right|^{-1} \left(\frac{\partial \mathbf{r}_c}{\partial x_1} \wedge \frac{\partial \mathbf{r}_c}{\partial x_2} \right). \quad (68)$$

We choose to parametrise the sheet in such a way that lines of constant x_1 and x_2 are lines of curvature⁴ of the centre-surface $\mathbf{r} = \mathbf{r}_c$ (see for example Kreyszig (1959)). This means that

$$\frac{\partial \mathbf{r}_c}{\partial x_1} \cdot \frac{\partial \mathbf{r}_c}{\partial x_2} = 0 \quad \text{and} \quad \frac{\partial^2 \mathbf{r}_c}{\partial x_1 \partial x_2} \cdot \mathbf{n} = 0,$$

so that the first and second fundamental forms of the surface are both diagonal. We put

$$a_1 = \left| \frac{\partial \mathbf{r}_c}{\partial x_1} \right|, \quad a_2 = \left| \frac{\partial \mathbf{r}_c}{\partial x_2} \right| \quad (69)$$

⁴At an umbilic point of the surface, where the principal curvatures are equal, these lines are not uniquely defined and at an isolated umbilic our model will possess spurious singular solutions.

and then we may define an orthonormal basis $\{\mathbf{e}_1, \mathbf{e}_2, \mathbf{n}\}$, where

$$\mathbf{e}_1 = \frac{1}{a_1} \frac{\partial \mathbf{r}_c}{\partial x_1} \text{ and } \mathbf{e}_2 = \frac{1}{a_2} \frac{\partial \mathbf{r}_c}{\partial x_2}. \quad (70)$$

We note the following three identities linking a_1 and a_2 to the principal curvatures of the centre-surface, κ_1 and κ_2 (the first is the so-called equation of Gauss):

$$\frac{\partial}{\partial x_1} \left(\frac{1}{a_1} \frac{\partial a_2}{\partial x_1} \right) + \frac{\partial}{\partial x_2} \left(\frac{1}{a_2} \frac{\partial a_1}{\partial x_2} \right) + a_1 a_2 \kappa_1 \kappa_2 = 0, \quad (71)$$

$$a_1 \frac{\partial \kappa_1}{\partial x_2} = (\kappa_2 - \kappa_1) \frac{\partial a_1}{\partial x_2}, \quad (72)$$

$$a_2 \frac{\partial \kappa_2}{\partial x_1} = (\kappa_1 - \kappa_2) \frac{\partial a_2}{\partial x_1}. \quad (73)$$

We use the coordinates (x_1, x_2, n) to describe a general point of the fluid sheet whose position is given by

$$\mathbf{r} = \mathbf{r}_c + n\mathbf{n}. \quad (74)$$

It is easily verified that, because of our choice that x_1 and x_2 parametrise lines of curvature of the centre-surface $\mathbf{r} = \mathbf{r}_c$, this coordinate system is orthogonal. This means that the Stokes equations and appropriate boundary conditions on the two free surfaces $n = \pm \frac{1}{2}h$ may be written down relatively easily. Then our asymptotic analysis is based on the assumptions (equivalent to those of section 2.3) that the thickness of the sheet is of order ϵL , while the curvature is of order L^{-1} , where L is a typical lengthscale. The leading-order equations are derived in detail in Howell (1994), and applied to the motion of a viscous sheet under an applied pressure drop in van de Fliert *et al.* (1995). Denoting by u_1 and u_2 the velocity components in the \mathbf{e}_1 - and \mathbf{e}_2 -directions *relative to the velocity of the centre-surface*, the leading-order stresses in the sheet are given by

$$\sigma_{11} = \frac{2h}{a_1 a_2} \left[2 \left(a_2 \frac{\partial a_1}{\partial t} + u_2 \frac{\partial a_1}{\partial x_2} + a_2 \frac{\partial u_1}{\partial x_1} \right) + \left(a_1 \frac{\partial a_2}{\partial t} + u_1 \frac{\partial a_2}{\partial x_1} + a_1 \frac{\partial u_2}{\partial x_2} \right) \right], \quad (75)$$

$$\sigma_{22} = \frac{2h}{a_1 a_2} \left[\left(a_2 \frac{\partial a_1}{\partial t} + u_2 \frac{\partial a_1}{\partial x_2} + a_2 \frac{\partial u_1}{\partial x_1} \right) + 2 \left(a_1 \frac{\partial a_2}{\partial t} + u_1 \frac{\partial a_2}{\partial x_1} + a_1 \frac{\partial u_2}{\partial x_2} \right) \right], \quad (76)$$

$$\bar{\sigma}_{12} = \frac{h}{a_1 a_2} \left[a_1 \frac{\partial u_1}{\partial x_2} + a_2 \frac{\partial u_2}{\partial x_1} \right]. \quad (77)$$

In terms of these, the leading-order equations may be written

$$\frac{\partial}{\partial t}(a_1 a_2 h) + \frac{\partial}{\partial x_1}(u_1 a_2 h) + \frac{\partial}{\partial x_2}(u_2 a_1 h) = 0, \quad (78)$$

representing conservation of mass,

$$\frac{\partial}{\partial x_1}(a_2 \sigma_{11}) + \frac{\partial}{\partial x_2}(a_1 \sigma_{12}) + \frac{\partial a_1}{\partial x_2} \sigma_{12} - \frac{\partial a_2}{\partial x_1} \sigma_{22} = 0, \quad (79)$$

and

$$\frac{\partial}{\partial x_1}(a_2\sigma_{12}) + \frac{\partial}{\partial x_2}(a_1\sigma_{22}) + \frac{\partial a_2}{\partial x_1}\sigma_{12} - \frac{\partial a_1}{\partial x_2}\sigma_{11} = 0, \quad (80)$$

representing force balances in the x_1 - and x_2 - directions, and a normal force balance,

$$\kappa_1\sigma_{11} + \kappa_2\sigma_{22} = 0. \quad (81)$$

Equations (71 – 73), (78 – 81) form a closed system for the unknowns h , u_1 , u_2 , a_1 , a_2 , κ_1 and κ_2 . Equations (79 – 81) are identical to the equations of linear shell theory. However, in our formulation the geometry is not prescribed; it must be found from coupled evolution equations. This is made clearer by reference to the following possible solution procedure:

- suppose the geometry of the sheet is known at some instant of time, that is h , a_1 , a_2 , κ_1 and κ_2 are all known functions of x_1 and x_2 ;
- solve (79 – 81) for σ_{11} , σ_{12} and σ_{22} by usual shell theory methods;
- update the geometry using the evolution equations (75 – 78). This last step will require use of the remaining identities.

In general, the solution of these equations is hampered by the dependence of the geometry on time. One aspect of this is that the form of the coordinate system is not known in advance. However, some analytical progress can be made when some symmetries of the geometry are preserved as the sheet evolves; examples of this may be found in Howell (1994) and van de Fliert *et al.* (1995).

4.4 Discussion of short-timescale behaviour for three-dimensional sheets

Consider the two-dimensional restriction of the equations of the section 4.3, found by setting

$$a_1 = a_2 = 1, \quad \kappa_2 = u_2 = \frac{\partial}{\partial x_2} = 0.$$

The choice $a_1 = 1$ means that x_1 may be identified with arc length s , and the leading-order equations are found to be

$$\frac{\partial h}{\partial t} + \frac{\partial}{\partial s}(u_1 h) = 0, \quad (82)$$

$$4\mu h \frac{\partial u_1}{\partial s} \kappa = 0, \quad (83)$$

$$\frac{\partial}{\partial s} \left(4\mu h \frac{\partial u_1}{\partial s} \right) = 0. \quad (84)$$

This system gives either $\kappa = 0$ (so that the sheet is straight) plus the Trouton model for h and u_1 , or if κ is nonzero then $u_1 = 0$, $h_t = 0$ and it is necessary to proceed further with the expansions to find an expression for κ (this is analogous to the large curvature analysis of section 2.3). The physical implication is that a two-dimensional sheet may

be bent into any shape desired *without inducing any leading-order tension in the sheet*. Leading-order tensions only occur once the sheet has straightened and it starts to stretch, satisfying the Trouton model.

We may now ask whether the sheets of more general geometry discussed in this section may exhibit some short-timescale behaviour. We should first note the following important difference between a two-dimensional sheet and a fully three-dimensional sheet: a two-dimensional sheet may be bent into any desired shape of the same length without any stretching, while given an arbitrary surface, there is a limited class of surfaces into which it can be deformed without stretching — the surfaces to which it is *isometric*. For example, a planar sheet can only be deformed without stretching into a surface which is *developable*.

We therefore conjecture that over a short timescale, a sheet of arbitrary initial shape will evolve to another surface to which it is isometric. The shape of this surface is determined by the forces acting on the sheet (contrast, for example, a two-dimensional sheet placed under tension by pulling its ends apart which will straighten, with a two-dimensional sheet acting under a pressure drop which will form a circular arc — see van de Fliert *et al.* (1995) for details). Once it has adopted this shape, stretching will commence and the equations of section 4.3 will then apply.

Of course, in order to examine the short-timescale behaviour more explicitly, it is likely that inertia effects will have to be included in the analysis, as they were for a two-dimensional sheet in section 3. It appears that the same dominant length- and timescales would result from such an analysis, with two main extra complications introduced due to the three-dimensionality of the sheet. Firstly, unlike the tension in a two-dimensional sheet, the stresses are functions of x and y as well as t ; this means that we may expect different parts of the sheet to respond over different length- and timescales. Secondly, we have seen that at each point of the sheet there is an associated direction of least stability; this ceases to be an issue in the purely two-dimensional case.

5 Conclusions

We have used systematic perturbation techniques to derive leading-order equations governing the dynamics of thin viscous sheets. The main results of this paper are (i) the identification of the relevant length- and timescales for the buckling of viscous sheets, (ii) the derivation of new models for fully three-dimensional sheets of arbitrary geometry.

Though the Trouton model, *i.e.* equations (10) and (13), can be written down very easily using heuristic mass- and force-balance arguments, our systematic approach pays dividends in the more complicated scenarios which follow, in which it is necessary to identify different lengthscales and timescales depending on the relative sizes of the inverse aspect ratio, the Reynolds number and the dimensionless curvature of the sheet. The complex three-dimensional geometry allowed for in the theory of section 4 makes heuristic physical arguments cumbersome and unconvincing.

There are other potentially important physical effects that we have neglected completely. Gravity, surface tension and non-constant viscosity can easily be incorporated into our models; this has been carried out by Howell (1994) and some details of the surface tension calculations are given in the appendix. The inclusion of inertia in the “viscous

shell” equations of section 4.3 is also considered by Howell (1994) and van de Fliert *et al.* (1995). In order to be applicable to diverse industrial processes, the theory could be extended to allow for coupled heat transfer, as well as more complicated rheology than incompressible Newtonian fluid; in principle our methods should still allow simplified leading-order equations to be derived.

Acknowledgements

I would like to thank Dr J.R. Ockendon, Mr D. Gelder, Prof. H.K. Moffatt and Dr S.D. Howison for their helpful advice, and Prof. B. Tchavdarov and Prof. S. Radev for some stimulating discussions. Part of this work was carried out with the financial support of SERC (now EPSRC).

References

- T.B. Benjamin & T. Mullin, 1988 Buckling instabilities in layers of viscous liquid subjected to shearing, *J. Fluid Mech.*, **195**, 523–540.
- J.D. Buckmaster, A. Nachman & L. Ting, 1975 The buckling and stretching of a viscida, *J. Fluid Mech.*, **69**, 1–20.
- J.N. Dewynne, J.R. Ockendon & P. Wilmott, 1989 On a mathematical model for fiber tapering, *SIAM J. Appl. Math.*, **49**, 983–990.
- J.N. Dewynne, J.R. Ockendon & P. Wilmott, 1992 A systematic derivation of the leading-order equations for extensional flows in slender geometries, *J. Fluid Mech.*, **244**, 323–338.
- J.N. Dewynne, P.D. Howell & P. Wilmott, 1994 Slender viscous fibres with inertia and gravity, *Quart. J. Mech. Appl. Math.*, **47**, 541–555.
- J. Eggers, 1993 Universal pinching of 3D axisymmetric free-surface flow, *Phys. Rev. Lett.*, **71**, 3458–3460.
- B.W. van de Fliert, P.D. Howell & J.R. Ockendon, 1995 Pressure-driven flow of a thin viscous sheet, *J. Fluid Mech.*, **292**, 359–376.
- P.D. Howell, 1994 Extensional thin layer flows, D.Phil. thesis, University of Oxford.
- M.P. Ida & M.J. Miksis, 1995 Dynamics of a lamella in a capillary tube, *SIAM J. Appl. Math.*, (to appear).
- E. Kreyszig, 1959 *Differential geometry*, University of Toronto Press (reprinted Dover, 1991).
- A.E.H. Love, 1927 *A treatise on the mathematical theory of elasticity*, Cambridge University Press.
- T.G. Myers, 1995 Thin films with high surface tension, OCIAM report, University of

Oxford.

J.R.A. Pearson & C.J.S. Petrie, 1970 The flow of a tubular film. Part 1. Formal mathematical representation, *J. Fluid Mech.*, **40**, 1–19.

J.R.A. Pearson & C.J.S. Petrie, 1970 The flow of a tubular film. Part 2. Interpretation of the model and discussion of solutions, *J. Fluid Mech.*, **42**, 609–625.

W.W. Schultz & S.H. Davis, 1982 One-dimensional liquid fibers, *Journal of Rheology*, **26**, 331–345.

L. Ting & J.B. Keller, 1990 Slender jets and sheets with surface tension, *SIAM J. Appl. Math.*, **50**, 1533–1546.

P. Wilmott, 1989 The stretching of a thin viscous inclusion and the drawing of glass sheets, *Phys. Fluids A*, **1**, 1098–1103.

A.L. Yarin, P. Gospodinov, & V.I. Roussinov, 1994 Stability loss and sensitivity in hollow-fiber drawing, *Phys. Fluids*, **6**, 1454–1463.

A.L. Yarin & B. Tchavdarov, 1994 Folding of plane liquid films, in preparation.

Appendix

Surface tension effects

All of the models presented in this paper may be generalised to include the effect of surface tension with relative ease. For example, in the case of a two-dimensional sheet considered in section 2.1, this is accomplished by replacing the zero-stress boundary conditions (6) and (7) by balances between the viscous stresses in the fluid and the surface tension forces, which are proportional to the curvatures of the two free surfaces. These take the nondimensionalised form,

$$\epsilon^2 \left(-p + 2u_x \mp \tilde{\gamma}(H_{xx} \pm \tfrac{1}{2}h_{xx}) \right) \left(H_x \pm \tfrac{1}{2}h_x \right) = u_y + \epsilon^2 v_x \quad \text{on } y = H \pm \tfrac{1}{2}h, \quad (85)$$

$$(u_y + \epsilon^2 v_x) \left(H_x \pm \tfrac{1}{2}h_x \right) = -p + 2v_y \mp \tilde{\gamma}(H_{xx} \pm \tfrac{1}{2}h_{xx}) \quad \text{on } y = H \pm \tfrac{1}{2}h, \quad (86)$$

where $\tilde{\gamma}$ is the dimensionless surface tension coefficient, given in terms of the dimensional coefficient γ by

$$\tilde{\gamma} = \frac{\epsilon\gamma}{\mu U}. \quad (87)$$

The analysis of section 2.1 may now be followed fairly closely; indeed, the asymptotic expansions need not be carried so far since the leading-order equations give (dropping subscripts)

$$\tilde{\gamma}H_{xx} = 0, \quad (88)$$

for the leading-order centre-line. The usual conservation of mass relation is also obtained,

$$h_t + (uh)_x = 0, \quad (89)$$

as well as an axial momentum balance with an extra contribution due to surface tension, namely

$$(4hu_x)_x + \frac{1}{2}\tilde{\gamma}hh_{xxx} = 0, \quad (90)$$

(inertia may be included in the model by incorporating the term multiplying the Reynolds number in (37) in the obvious way).

This model might apply to a very thin film, whose geometry is dominated by surface tension via (88). It may be contrasted with the so-called lubrication equation,

$$h_t + (h^3h_{xxx})_x = 0, \quad (91)$$

which applies to the surface tension-dominated flow of a thin viscous film over a rigid substrate; see Myers (1995) for details.

The model may also be contrasted with the corresponding equations governing the stretching of an axisymmetric fibre with surface tension, namely

$$(R^2)_t + (uR^2)_x = 0, \quad (3R^2u_x + \gamma^*R)_x = 0, \quad (92)$$

where R is the fibre radius, u the axial velocity and

$$\gamma^* = \frac{\gamma}{\epsilon\mu U}. \quad (93)$$

Notice that surface tension effects are felt much more strongly by a slender fibre due to the high curvature of the free surface in the plane orthogonal to the fibre's axis; this motivates the rescaling of the surface tension coefficient. This also expresses itself through the fact that (92) admits solutions in which the fibre breaks up in finite time; see Eggers (1993). Whether the same can be said about (90) or (91) remains an open question.

If the scaling (93) is applied to a two-dimensional sheet then surface tension effects only enter the centre-line equation, which becomes (including inertia also)

$$(Rehu^2 - 4hu_x - \gamma^*)H_{xx} + 2RehuH_{xt} + RehH_{tt} = 0, \quad (94)$$

while h and u are governed by (37). The discriminant of this equation is now $Reh(4u_x + \gamma^*)$, so that surface tension has a stabilising effect, tending to counter the change in type from hyperbolic to elliptic when the sheet is under compression.

In extending the above to three-dimensional sheets, we employ the scaling (93) which is more relevant for viscosity-dominated flows such as in glass sheets, while (87) is more applicable to surface tension-dominated films, for example the lamellae in a foam (see Ida & Miksis (1995) for such an application). After this choice of scaling, surface tension effects are found to enter the models only through the centre-line equation, where they contribute to the tension in the sheet. For example (55) becomes

$$(2h(2u_x + v_y) + \gamma^*)H_{xx} + 2h(u_y + v_x)H_{xy} + (2h(u_x + 2v_y) + \gamma^*)H_{yy} = 0, \quad (95)$$

and the left-hand side of (62) is altered similarly, while (81) becomes

$$\kappa_1(\sigma_{11} + \gamma^*) + \kappa_2(\sigma_{22} + \gamma^*) = 0. \quad (96)$$

Erratum

I have discovered a mistake in the paper

HOWELL, P.D. (1996) Models for thin viscous sheets. *Euro. J. Appl. Maths* **7**, 321–343,

namely that equation (77) should read

$$\bar{\sigma}_{12} = \frac{h}{a_1 a_2} \left[a_1 \frac{\partial u_1}{\partial x_2} - u_1 \frac{\partial a_1}{\partial x_2} + a_2 \frac{\partial u_2}{\partial x_1} - u_2 \frac{\partial a_2}{\partial x_1} \right]. \quad (77)$$

This error also appears in the earlier paper

VAN DE FLIERT, B.W., HOWELL, P.D. & OCKENDON, J.R. (1995) Pressure-driven flow of a thin viscous sheet. *J. Fluid Mech.* **292**, 359–376.

It was not previously discovered because the two missing terms are identically zero in all the special cases considered in the latter paper.

Peter Howell
Mathematical Institute
24–29 St Giles’
Oxford OX1 3LB
27 November 1997